Received 11 July 2017; revised 8 August 2017; accepted 6 September 2017. Date of publication 13 September 2017; date of current version 24 October 2017. The review of this paper was arranged by Editor U. Perera.

Digital Object Identifier 10.1109/JEDS.2017.2751651

Circular Structure for High Mechanical Bending Stability of a-IGZO TFTs

MALLORY MATIVENGA (Member, IEEE), HAEYEON JUN, YOUNWOO CHOE, JAE GWANG UM (Student Member, IEEE), AND JIN JANG (Member, IEEE)

Advanced Display Research Center, Department of Information Display, Kyung Hee University, Seoul 130-701, South Korea

CORRESPONDING AUTHOR: M. MATIVENGA (e-mail: mallorykr@gmail.com)

This work was supported by the National Research Foundation of Korea (NRF) through the Korea Government under Grant NRF2016R1C1B1015765.

ABSTRACT We employ a circular (Corbino) thin-film transistor (TFT) structure, in which the outer-ring is the drain and the inner-ring is the source, to improve the stability of amorphous–indium–gallium–zinc–oxide TFTs under tensile bending strain. We attribute the stability improvement to a more uniform electric field distribution across the circular channel, as it is isolated from local electric field crowding at sharp corners or channel edges. In addition, the effect of strain-induced increase in channel charge concentration is small in Corbino TFTs, owing to the larger outer-ring electrode, which depletes more electrons than the drain of rectangular TFTs. Furthermore, the circular shape results in bending direction independence, which is very important in multi-TFT circuits, where TFT orientation varies with position.

INDEX TERMS Circular, Corbino, flexible, IGZO, strain, TFT.

I. INTRODUCTION

A major challenge in thin-film transistor (TFT)-based flexible electronics is the development of a TFT that is stable under mechanical bending strain [1], [2]. Stability enhancement techniques commonly applied to TFTs built on rigid substrates, such as glass; do not always apply to TFTs on flexible substrates, such as plastic. For instance, high temperature deposition or annealing of materials making up the TFT stack improves TFT stability, but neither the latter nor the former can be applied to TFTs on plastic because of the temperature restrictions imposed by plastic substrates [3], [4]. Amorphous oxide semiconductors (AOSs), such as amorphous-indium-gallium-zinc-oxide (a-IGZO), have thus become potential candidates for flexible TFT channel materials, given that they exhibit high performance, even when deposited at low-temperature [5]–[10].

Despite their high performance, conventional AOS TFTs with rectangular shaped electrodes and semiconductor islands degrade significantly under mechanical bending strain [11]–[14]. Several research and experimental studies have thus been devoted to finding ways of improving their mechanical bending stability, which include the use of double-gate TFT structures [15], ultrathin substrates [16], [17], nanowires [18], mesh and strip patterning of device layers [19] and locating them close to the neutral bending plane [18]. However, further improvements are still required, as most of these techniques do not address the bending direction dependence that is inherent in most rectangular (Fig. 1(a)) TFT structures [19] and the detrimental effects of stress concentrated points, local electric field crowding or spreading current that is characteristic of irregular channel layers with sharp corners or channel edges [20]. Here we investigate the effect of a circular TFT structure (Fig. 1(b)), also known as the Corbino TFT structure [21]–[24] on the mechanical bending stability of a-IGZO TFTs. We compare the performance of Corbino a-IGZO TFTs to that of the conventionally rectangular shaped a-IGZO TFTs under tensile bending strain.

II. EXPERIMENT

Rectangular shaped TFTs (Fig. 1(a)) and Corbino TFTs (Fig. 1(b)) with the back channel etched inverted staggered structure are fabricated simultaneously on a 15 μm-thick plastic substrate, polyimide (PI), using carrier glass coated with a 1 nm-thick layer of mixed carbon nanotubes (CNTs) and graphene oxide (GO), as explained in

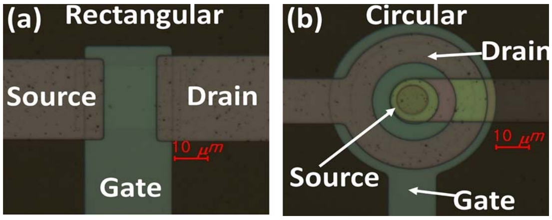

FIGURE 1. Optical micrographs of fabricated TFTs. (a) Rectangular. (b) Circular.

detail elsewhere [25]. The carrier glass is for mechanical support during fabrication and the CNT/GO layer minimizes the adhesion of the PI to glass, which allows mechanical detachment from the glass when the fabrication process is complete. Furthermore, because the CNT/GO layer remains embedded to the backside of the PI substrate after detachment from glass, it protects the TFTs from electrostatic discharge (ESD) because of the conductive CNT and it provides mechanical support to the flexible substrate – preventing it from wrinkling or curling [25]. We chose PI for its lower coefficient of thermal expansion (CTE), higher chemical resistance, and higher continuous processing temperature, compared to other polymer substrates. The gate insulator (250 nm) and passivation layer (300 nm) are SiO_2, layers deposited by plasma-enhanced chemical vapor deposition (PECVD) at 300°C and the gate (60 nm) and source/drain (120 nm) electrodes are made of sputter deposited molybdenum. The a-IGZO layer is 20 nm thick and sputter deposited at 200°C, using a polycrystalline IGZO target (In_2O_3: Ga_2O_3: ZnO = 1: 1: 1 mol%) at 200°C, in Ar:O_2 gas ratio set at 4:8. The chemical composition of the deposited a-IGZO is determined to be In:Ga:Zn = 3:2:1 in atomic ratio.

After fabrication, the TFTs undergo thermal annealing at 250°C in vacuum for 2 h to achieve a reproducible unstressed state, after which they are mechanically detached from the carrier glass. First, we measure the TFT characteristics in their initial flat state before any bending tests and repeat the same measurements, while bending the samples to cylinders with a radius of 2 mm. Then, we measure the TFTs in the flat state after bending to check if the TFT characteristics recover from the effects of strain. We also obtain two sets of these measurements; (1) when the bending axis is parallel to the flow of current from source to drain and (2) when the bending axis is perpendicular to the flow of current. This allows testing the bending direction dependency of the devices.

We apply the tensile strain by rolling the samples with the TFT side facing upwards to cylinders with a radius of 2 mm. Given that the total device thicknesses (d_f) is ~855 nm, which is much smaller than that of the substrate (d_s = 15μm), the strain on the top surface of the samples ($\varepsilon_{surface}$) can be approximated by $\varepsilon_{surface} = (d_s + d_f)/2R$, where R is the bending radius. For R = 2 mm, the corresponding tensile strain applied to the top surface is ~0.4%. The TFT's turn-on voltage (V_{ON}), which is taken as the

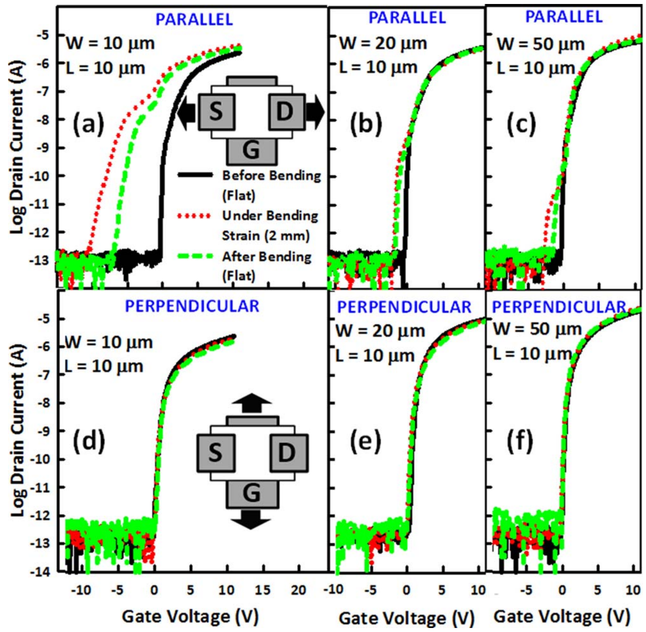

FIGURE 2. Rectangular TFT transfer characteristics measured before, during and after the application of stress in the direction (a-c) parallel and (d-f) perpendicular to the flow of current for fixed L = 10 μm and varying W. Insets of (a) and (d) show the direction of tensile strain.

gate voltage (V_{GS}) at which the drain current (I_{DS}) starts to monotonically increase, is used for characterization. For corbino TFTs, channel length (L) is given by $R_2 - R_1$, where R_1 and R_2 are respectively the radii of the inner and outer ring electrodes and when the drain voltage $V_{DS} < V_{GS} - V_{ON}$, the effective channel width (W) is estimated from $W/L = 2\pi/\ln(R_2/R_1)$ [21]. The field-effect mobility (μ_{FE},), derived from transconductance (g_M), $\partial I_{DS}/\partial V_{GS}$, is given by $\mu_{FE(g_M L)/(WV_{DS}C_{OX})}$, where C_{OX} = ~1.32 x 10^{-8} F/cm^2 is the gate-insulator capacitance per unit area and V_{DS} = 0.1 V. The substhreshold swing (SS) is taken as (d log (I_{DS})/d $V_{GS})^{-1}$ of the range 10 pA = I_{DS} =100 pA, with V_{DS} = 0.1 V.

III. RESULTS AND DISCUSSION

Fig. 2 and Fig. 3 show typical bending tests results for rectangular and Corbino TFTs. Fig. 4 summarizes device parameters extracted for several Corbino and rectangular TFTs. For rectangular TFTs, it is evident that tensile strain applied in the direction parallel to the channel (Fig. 2(a-c)) has more effect than that applied in the direction perpendicular to the channel (Fig. 2(d-f)). Under bending tensile strain that is parallel to the channel, the negative V_{ON} shift (ΔV_{ON}) experienced by the rectangular TFTs increases with decreasing W for fixed L (Fig. 2(a-c)). In the flat state, TFT transfer characteristics recover towards their initial state, but not completely. As there are no visible cracks after bending, it is reasonable to conclude that tensile bending strain, in this case, does not result in cracking because cracks cause device breakdown, which is not recoverable by thermal annealing. Rather, the results imply that tensile bending strain induces

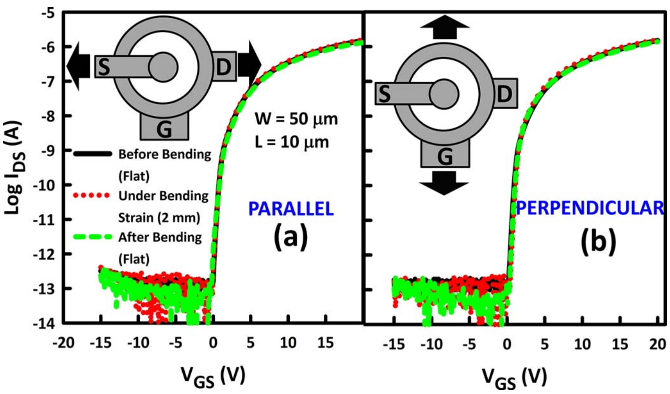

FIGURE 3. Circular TFT transfer characteristics measured before, during and after the application of stress in the direction (a) parallel and (d) perpendicular to the flow of current. Insets show the direction of tensile strain.

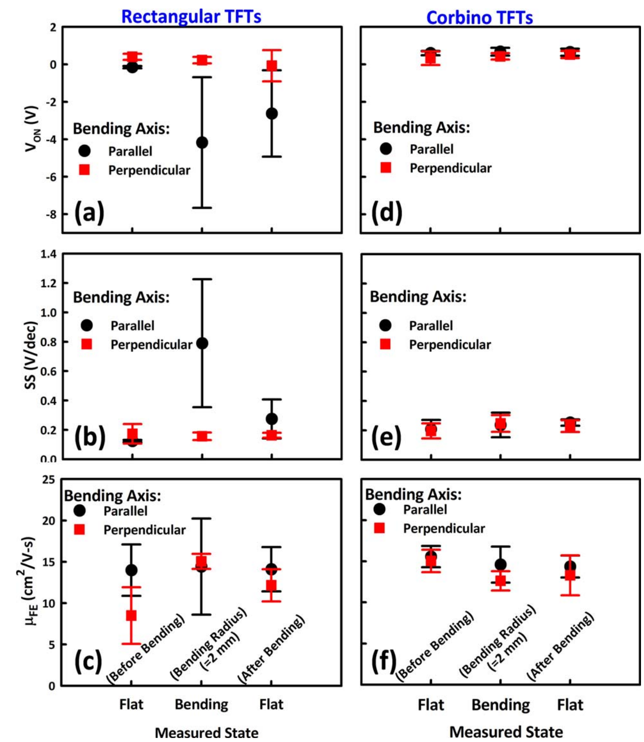

FIGURE 4. Effects of tensile bending strain on rectangular and Corbino TFT parameters obtained from testing several devices. Turn-on voltage (V_{ON}), subthreshold swing (SS), and field-effect mobility (μ_{FE}) for (a-c) rectangular and (d-f) Corbino TFTs. Symbols represents the means and error bars are the standard deviations from the means.

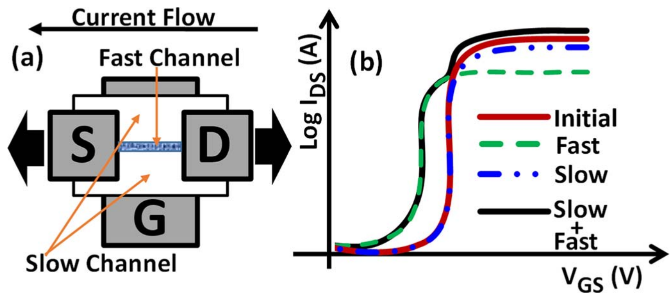

FIGURE 5. Hump mechanism: (a) Formation of a strain-induced Fast channel, localized along the bending axis. (b) Schematic TFT transfer characteristics showing how two logical channels, *slow* channel and *fast* channel, sum up to form transfer characteristics with a "hump".

the formation of metastable defects. These defects should be carrier donors in nature, as they result in negative ΔV_{ON}, which indicates a shifting of the Fermi level (E_F) closer to the conduction band (E_C) due to increase in carrier concentration (N_D). In addition, the defects dominantly occur in the a-IGZO layer, as there is no significant increase in gate leakage current. Note that an increase in gate leakage current is a direct indicate of gate-insulator degradation.

Consistent with previously reports, tensile bending may strain metal-oxide bonds in AOSs, resulting in the formation of oxygen vacancies, which act as donors in the AOSs [20]. Recent reports have verified through TCAD device simulation that the negative ΔV_{ON} experienced by a-IGZO TFTs under tensile bending strain is due to an increase in N_D [15], [26], [27]. Application of strain in the direction perpendicular to the channel, however, induces a very small negative ΔV_{ON}, and TFT characteristics recover completely when measured again in the flat state (Fig. 2(d-f)). As this dependency of the degradation of TFT characteristics on bending direction (Fig. 4(a)-(c)) is a common occurrence in rectangular TFTs [19], [27], [28], it warrants investigation. The increase in N_D should be, to some extent, localized along the bending axis. In the case of parallel bending, this localized region of high N_D, is physically connected to both the source to drain electrodes, thereby forming an additional low resistance current path (Fig. 5(a)); hence the negative ΔV_{ON}. In the case of perpendicular bending, the region of high N_D is isolated from the source and drain, as it runs along the W-direction, and thus forms no additional current paths and consequently no ΔV_{ON}. In both cases, the generated donors are metastable in nature; otherwise, the TFT characteristics would not recover after bending. In addition, the generated donors, extend only slightly along the direction perpendicular to the bending axis, otherwise lateral diffusion would result in the same TFT performance for both bending directions.

In the case of parallel bending, it is reasonable to assume a smaller width for the region with high N_D compared to the rest of the channel (Fig. 5(a)). The "hump" that occurs in the transfer characteristics of the rectangular TFTs after application of parallel bending strain, supports this supposition because it decreases in magnitude with increasing W (Fig. 2(a-c)). It is known that the formation of two logical channels in one physical device causes a "hump" in TFT transfer characteristics, if the two logical channels have different resistances and different widths [29]–[33]. Similarly, parallel bending results in the formation of two logical channels; 1) 'Fast-Channel' – a low resistance channel along the localized region of high N_D and 2) 'Slow-Channel' – the rest of the channel that is not significantly affected by strain (Fig. 5(a)). Fast-Channel turns ON before Slow-Channel because the E_F of the former is closer to E_C than

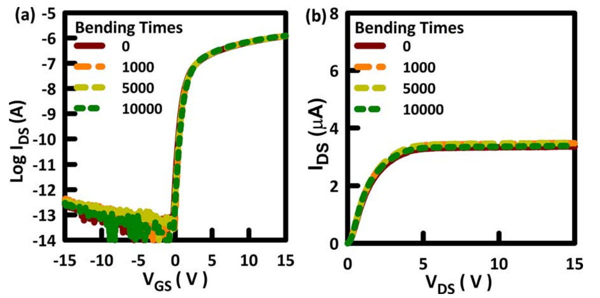

FIGURE 6. Effects of repeated tensile bending cycles on Corbino TFTs: (a) Transfer characteristics and (b) output characteristics. Bending radius was 0.48 mm and the TFT channel width and length were 50 and 10 μm, respectively.

that of the latter. However, because the effective width of Fast-Channel is smaller than that of Slow-Channel, the former has lower I_{DS} than the latter. The sum of the currents from these two channels yields a transfer curve that exhibits a "hump" in the subthreshold region (Fig. 5(b)). Note that when W increases, the W of "Fast channel" remains the same, while that of "Slow channel" increases. This explains why the "hump" decreases in magnitude with increasing W. Carriers generated during the application of tensile strain diffuse laterally when the TFTs return to their flat state. This is the reason why the size of the "hump" decreases when the TFT characteristics are measured in the flat state after bending (Fig. 2(a)-(c)). In cases where the TFTs are measured in the flat state after repeated "bending" and "flat" cycles, uniform carrier distribution can be achieved such that TFT characteristics exhibit negative ΔV_{ON} , without a hump [29].

Corbino TFTs, on the other hand, do not only show bending direction independence (Fig. 3), but also exhibit better mechanical stability compared to the rectangular TFTs under parallel bending strain (Fig. 4). Note that the degradation of Corbino TFTs should be similar to that of the rectangular TFTs under parallel bending, but by comparing results in Fig. 2(c) and Fig. 3(a), it is evident that Corbino TFTs exhibit better stability compared to rectangular TFTs with an equivalent channel size. The Corbino TFTs are measured with the outer ring biased as the drain because in this configuration, they exhibit infinite output resistance beyond pinch-off, which is important in applications where TFTs play the role of current drivers, as reported elsewhere [22]. In all measurements, the source is thus grounded, making the effect of the source-to-drain overlap (Fig. 1(b)) insignificant.

The Corbino TFTs also showed excellent mechanical durability even when exposed to 10,000 bending cycles (Fig. 6). Using an automated bending machine [19], we could repeatedly bent to the TFTs to a radius of 0.48 mm, which corresponds to tensile strain of ∼1.65%. Compared to rectangular TFTs, the better stability exhibited by the Corbino TFTs can be attributed to a more uniform electric field distribution across the circular channel, as it is isolated from local electric-field crowding at sharp corners or channel edges [34]. Under bending strain, sharp corners or edges can be a source of stress concentrations, and their isolation from the circular channel in Corbino TFTs improves the mechanical stability significantly. In addition, the flow of current in Corbino TFTs is thus immune to irregularly-shaped/unpatterned channel layers that are common in flexible TFTs, especially those printed from inks [35]. Furthermore, the effect of the strain-induced increase in carrier concentration is a lesser in Corbino than in rectangular TFTs, owing to the larger outer-ring electrode, which depletes more electrons than the drain of rectangular TFTs. The bending direction independence exhibited by the Corbino TFTs is very important in multi-TFT circuits, where TFT orientation varies with position.

IV. CONCLUSION

The Corbino TFT structure does not only provide bending direction independence, but also achieves better stability under mechanical bending strain compared to rectangular shaped TFTs. The bending direction independence is very important in multi-TFT circuits, where TFT orientation varies with position. Sharp corners or channel edges in rectangular TFTs always lead to local electric field crowding and leakage currents, which degrade TFT performance. The better stability exhibited by the Corbino TFTs results from a more uniform electric field distribution across the circular channel, as it is isolated any form of this electric field crowding.

REFERENCES

[1] H. Gleskova, S. Wagner, W. Soboyejo, and Z. Suo, "Electrical response of amorphous silicon thin-film transistors under mechanical strain," *J. Appl. Phys.*, vol. 92, no. 10, pp. 6224–6229, Oct. 2002.
[2] D. H. Kim *et al.*, "Stretchable and foldable silicon integrated circuits," *Nature*, vol. 320, no. 5875, pp. 507–511, Apr. 2008.
[3] M. D. H. Chowdhury, S. H. Ryu, P. Migliorato, and J. Jang, "Effect of annealing time on bias stress and light-induced instabilities in amorphous indium-gallium-zinc-oxide thin-film transistors," *J. Appl. Phys.*, vol. 110, no. 11, pp. 5–10, Dec. 2011.
[4] S. Khan, L. Lorenzelli, and R. S. Dahiya, "Technologies for printing sensors and electronics over large flexible substrates: A review," *IEEE Sensors J.*, vol. 15, no. 6, pp. 3164–3185, Jun. 2015.
[5] M. Nag *et al.*, "High performance a-IGZO thin-film transistors with mf-PVD SiO2 as an etch-stop-layer," *J. Soc. Inf. Display*, vol. 22, no. 1, pp. 23–28, Jan. 2014.
[6] E. Fortunato, P. Barquinha, and R. Martins, "Oxide semiconductor thin-film transistors: A review of recent advances," *Adv. Mater.*, vol. 24, no. 22, pp. 2945–2986, Jun. 2012.
[7] T. Kamiya, K. Nomura, and H. Hosono, "Origins of high mobility and low operation voltage of amorphous oxide TFTs: Electronic structure, electron transport, defects and doping*," *J. Display Technol.*, vol. 5, no. 7, pp. 273–288, Dec. 2009.
[8] K. Nomura *et al.*, "Room-temperature fabrication of transparent flexible thin-film transistors using amorphous oxide semiconductors," *Nature*, vol. 432, pp. 488–492, Jul. 2004.
[9] J. S. Lee, S. Chang, S.-M. Koo, and S. Y. Lee, "High-performance a-IGZO TFT with ZrO2 gate dielectric fabricated at room temperature," *IEEE Electron Device Lett.*, vol. 31, no. 3, pp. 225–227, Mar. 2010.
[10] H.-H. Hsu, C.-Y. Chang, and C.-H. Cheng, "A flexible IGZO thin-film transistor with stacked TiO2-based dielectrics fabricated at room temperature," *IEEE Electron Device Lett.*, vol. 34, no. 6, pp. 768–770, Jun. 2013.
[11] M.-J. Park *et al.*, "Improvements in the bending performance and bias stability of flexible InGaZnO thin film transistors and optimum barrier structures for plastic poly(ethylene naphthalate) substrates," *J. Mater. Chem. C*, vol. 3, no. 18, pp. 4779–4786, Apr. 2015.

[12] J.-S. Seo *et al.*, "Solution-processed flexible fluorine-doped indium zinc oxide thin-film transistors fabricated on plastic film at low temperature," *Sci. Rep.*, vol. 3, pp. 1–9, Jun. 2013.

[13] H. Oh, K. Cho, S. Park, and S. Kim, "Electrical characteristics of bendable a-IGZO thin-film transistors with split channels and top-gate structure," *Microelectron. Eng.*, vol. 159, pp. 179–183, Jun. 2016.

[14] H.-C. Lai, Z. Pei, J.-R. Jian, and B.-J. Tzeng, "Alumina nanoparticle/polymer nanocomposite dielectric for flexible amorphous indium-gallium-zinc oxide thin film transistors on plastic substrate with superior stability," *Appl. Phys. Lett.*, vol. 105, no. 3, pp. 1–5, Jul. 2014.

[15] X. Li *et al.*, "Highly robust flexible oxide thin-film transistors by bulk accumulation," *IEEE Electron Device Lett.*, vol. 36, no. 8, pp. 811–813, Aug. 2015.

[16] H. U. Li and T. N. Jackson, "Oxide semiconductor thin film transistors on thin solution-cast flexible substrates," *IEEE Electron Device Lett.*, vol. 36, no. 1, pp. 35–37, Jan. 2015.

[17] H. E. Lee *et al.*, "Skin-like oxide thin-film transistors for transparent displays," *Adv. Funct. Mater.*, vol. 26, no. 34, pp. 6170–6178, Sep. 2016.

[18] M. C. McAlpine, R. S. Friedman, and C. M. Lieber, "High-performance nanowire electronics and photonics and nanoscale patterning on flexible plastic substrates," *Proc. IEEE*, vol. 93, no. 7, pp. 1357–1363, Jul. 2005.

[19] S. Lee, D. Jeong, M. Mativenga, and J. Jang, "Highly robust bendable oxide thin-film transistors on polyimide substrates via mesh and strip patterning of device layers," *Adv. Funct. Mater.*, vol. 27, no. 29, Aug. 2017, Art. no. 1700437.

[20] T. Sekitani *et al.*, "Ultraflexible organic field-effect transistors embedded at a neutral strain position," *Appl. Phys. Lett.*, vol. 87, no. 17, pp. 1–3, Oct. 2005.

[21] T. Sekitani, U. Zschieschang, H. Klauk, and T. Someya, "Flexible organic transistors and circuits with extreme bending stability," *Nat. Mater.*, vol. 9, no. 12, pp. 1015–1022, 2010.

[22] N. Munzenrieder, K. H. Cherenack, and G. Troster, "The effects of mechanical bending and illumination on the performance of flexible IGZO TFTs," *IEEE Trans. Electron Devices*, vol. 58, no. 7, pp. 2041–2048, Jul. 2011.

[23] D. Munteanu, S. Cristoloveanu, and H. Hovel, "Circular pseudo−metal oxide semiconductor field effect transistor in silicon−on−insulator analytical model, simulation, and measurements," *Electrochem. Solid State Lett.*, vol. 2, no. 5, pp. 242–243, Feb. 1999.

[24] M. Mativenga *et al.*, "Infinite output resistance of Corbino thin-film transistors with an amorphous-InGaZnO active layer for large-area AMOLED displays," *IEEE Trans. Electron Devices*, vol. 61, no. 9, pp. 3199–3205, Sep. 2014.

[25] W.-C. Huang, S.-Y. Sun, C.-C. Cheng, C.-Y. Liu, and M.-F. Chiang, "A study on Corbino a-IGZO TFTs with different bending curvatures for flexible electronics," in *Proc. 22nd Int. Workshop IEEE Active Matrix Flatpanel Displays Devices (AM FPD)*, Kyoto, Japan, Jul. 2015, pp. 119–122.

[26] C. Zhao, T.-C. Fung, and J. Kanicki, "Half-Corbino short-channel amorphous In–Ga–Zn–O thin-film transistors with a-SiOx or a-SiOx/a-SiNx passivation layers," *Solid State Electron.*, vol. 120, pp. 25–31, Jun. 2016.

[27] M. Mativenga, D. Geng, B. Kim, and J. Jang, "Fully transparent and rollable electronics," *ACS Appl. Mater. Interfaces*, vol. 7, no. 3, pp. 1578–1585, Dec. 2015.

[28] M. M. Billah, M. M. Hasan, and J. Jang, "Effect of tensile and compressive bending stress on electrical performance of flexible a-IGZO TFTs," *IEEE Electron Device Lett.*, vol. 38, no. 7, pp. 890–893, Jul. 2017.

[29] M. M. Hasan, M. M. Billah, M. N. Naik, J. G. Um, and J. Jang, "Bending stress induced performance change in plastic oxide thin-film transistor and recovery by annealing at 300°C," *IEEE Electron Device Lett.*, vol. 38, no. 8, pp. 1035–1038, Aug. 2017, doi: 10.1109/LED.2017.2718565.

[30] M. H. Lee, B.-F. Hsieh, and S. T. Chang, "Electrical properties correlated with redistributed deep states in a-Si: H thin-film transistors on flexible substrates undergoing mechanical bending," *Thin Solid Films*, vol. 528, pp. 82–85, Apr. 2013.

[31] P. Sallagoity, M. Ada-Hanifi, M. Paoli, and M. Haond, "Analysis of width edge effects in advanced isolation schemes for deep submicron CMOS technologies," *IEEE Trans. Electron Devices*, vol. 43, no. 11, pp. 1900–1906, Nov. 1996.

[32] A. Valletta, P. Gaucci, L. Mariucci, G. Fortunato, and F. Templier, "'Hump' characteristics and edge effects in polysilicon thin film transistors," *J. Appl. Phys.*, vol. 104, no. 12, Dec. 2008, Art. no. 124511.

[33] M. Mativenga *et al.*, "Degradation model of self-heating effects in silicon-on-glass TFTs," *IEEE Trans. Electron Devices*, vol. 58, no. 8, pp. 2440–2447, Aug. 2011.

[34] M. Mativenga, M. Seok, and J. Jang, "Gate bias-stress induced hump-effect in transfer characteristics of amorphous-indium-galium-zinc-oxide thin-film transistors with various channel widths," *Appl. Phys. Lett.*, vol. 99, no. 12, Sep. 2011, Art. no. 122107.

[35] C.-F. Huang *et al.*, "Stress-induced hump effects of p-channel polycrystalline silicon thin-film transistors," *IEEE Electron Device Lett.*, vol. 29, no. 12, pp. 1332–1335, Dec. 2008.

[36] D. C. Mayer, R. C. Lacoe, E. E. King, and J. V. Osborn, "Reliability enhancement in high-performance MOSFETs by annular transistor design," *IEEE Trans. Nucl. Sci.*, vol. 51, no. 6, pp. 3615–3620, Dec. 2004.

[37] C. Avis, H. R. Hwang, and J. Jang, "Effect of channel layer thickness on the performance of indium–zinc–tin oxide thin film transistors manufactured by inkjet printing," *ACS Appl. Mater. Interfaces*, vol. 6, no. 14, pp. 10941–10945, May 2014.

MALLORY MATIVENGA (S'12–M'15) received the M.S. and Ph.D. degrees in information display engineering from Kyung Hee University, Seoul, South Korea, in 2010, and 2014, respectively. He is currently an Assistant Professor of information display with Kyung Hee University.

HAEYEON JUN received the B.S. degree in information display from Kyung Hee University, Seoul, South Korea, in 2017, where she is currently pursuing the M.S. degree in information display engineering. Her current research interests include Perovskite semiconductor-based transistors and light emitting diodes for use in sensor and display applications.

YOUNWOO CHOE received the B.S. degree in material physics from Dong-A University, Busan, South Korea, in 2015 and the M.S. degree in information display from Kyung Hee University, Seoul, South Korea, in 2017. Her current research interests include amorphous oxide semiconductor-based thin-film transistors for use in flexible display applications.

JAE GWANG UM (S'15) received the M.S. degree in information display engineering from Kyung Hee University, Seoul, South Korea, in 2013, where he is currently pursuing the Ph.D. degree in information display. His current research interests include amorphous oxide semiconductor-based thin-film transistors for use in display applications.

JIN JANG (M'94) received the Ph.D. degree in physics from the Korea Advanced Institute of Science and Technology, Seoul, South Korea, in 1982. He is currently a Professor of information display with Kyung Hee University, Seoul.